ORIGINAL ARTICLE

Deposition of Hyperphosphorylated Tau in Cerebellum of PS1 E280A Alzheimer's Disease

Diego Sepulveda-Falla, MD[1,2]; Jakob Matschke, MD[1]; Christian Bernreuther, MD, PhD[1];
Christian Hagel, MD[1]; Berta Puig, PhD[1]; Andres Villegas, MD, PhD[2]; Gloria Garcia, MSc[2]; Julian Zea, BSc[2];
Baltazar Gomez-Mancilla, MD, PhD[3]; Isidre Ferrer, MD[4]; Francisco Lopera, MD[2]; Markus Glatzel, MD[1]

[1] Institute of Neuropathology, University Medical Center Hamburg-Eppendorf, Hamburg, Germany.

[2] Neuroscience Group of Antioquia, Faculty of Medicine, University of Antioquia, Medellín, Colombia.

[3] Institutes for BioMedical Research, Neurosciences Discovery, Novartis Pharma AG, Basel, Switzerland.

[4] Pathologic Anatomy Service, Institute of Neuropathology, CIBERNED, IDIBELL-University Hospital of Bellvitge, L'Hospitalet de Llobregat, University of Barcelona, Spain.

Abstract

Early-onset familial Alzheimer's disease (AD) caused by presenilin-1 mutation E280A (PS1-E280A) presents wide clinical and neuropathological variabilities. We characterized clinically and neuropathologically PS1-E280A focusing in cerebellar involvement and compared it with early-onset sporadic Alzheimer's disease (EOSAD). Twelve E280A brains and 12 matched EOSAD brains were analyzed for beta-amyloid and hyperphosphorylated tau (pTau) morphology, beta-amyloid subspecies 1–40, 1–42 levels, pTau levels, and expression of stress kinases in frontal cortex and cerebellum. The data were correlated to clinical and genetic findings. We observed higher beta-amyloid load, beta-amyloid 1–42 and pTau concentrations in frontal cortex of PS1-E280A compared with EOSAD. High beta-amyloid load was found in the cerebellum of PS1-E280A and EOSAD patients. In PS1-E280A, beta-amyloid localized to the molecular and Purkinje cell layers, whereas EOSAD showed them in Purkinje and granular cell layers. Surprisingly, 11 out of 12 PS1-E280A patients showed deposition of pTau in the cerebellum. Also, seven out of 12 PS1-E280A patients presented cerebellar ataxia. We conclude that deposition of beta-amyloid in the cerebellum is prominent in early-onset AD irrespective of genetic or sporadic origin. The presence of pTau in cerebellum in PS1-E280A underscores the relevance of cerebellar involvement in AD and might be correlated to clinical phenotype.

INTRODUCTION

Alzheimer's disease (AD) is the most common neurodegenerative disease. Clinically, it is characterized by cognitive decline leading to severe dementia and death (7). Age is one of the most important risk factors (23). Approximately 1% to 6% of cases are defined as early-onset (before the age of 65) and nearly 70% of these are associated with mutations in amyloid precursor protein (APP), presenilin-1 (PS1) or presenilin-2 (PS2) genes (4). Late-onset AD (after the age of 65) has not been associated with a single genetic trait; however, allele 4 of apolipoprotein E (ApoE) has shown to be a genetic risk factor and ~40% of these patients show at least one ApoE4 allele (6).

Definite diagnosis of AD can only be made postmortem. The neuropathological hallmarks of the disease include brain atrophy, extracellular deposition of beta amyloid (Aβ) and neurofibrillary tangles (24). Aβ is a 38 to 42 amino acid long peptide resulting from sequential cleavage of APP (44). Neurofibrillary tangles (NFT) or neuropil threads and dystrophic neurites result from the intracellular accumulation of hyperphosphorylated tau (pTau), a microtubule-associated protein (22).

The PS1 gene is located on chromosome 14q24.3 and its mutations are the most common cause of early-onset familial AD (EOFAD). More than 160 pathogenic mutations have been identified in the PS1 gene (http://www.molgen.ua.ac.be/ADMutations) (38). PS1 is part of the gamma secretase complex and acts together with beta secretase to generate Aβ from APP via the amyloidogenic pathway (39).

Mutations in PS1 affect APP processing, shifting the ratio between the production of $A\beta_{42}/A\beta_{40}$ toward the longer, more aggregation-prone $A\beta_{42}$ (9). The neuropathological phenotype of EOFAD with mutations in PS1 is diverse. Common features include abundant deposits of $A\beta_{42}$ and pTau, prominent atrophy and neuronal loss. Some PS1 mutations show large diffuse

Aβ_{42}-rich cotton wool plaques (38), others show cerebellar amyloid deposits (32) and one distinct PS1 mutation is characterised by Pick-type tauopathy in the absence of Aβ (12).

Clinically, PS1 EOFAD is characterized by variable yet early disease onset and high penetrance (31). This phenotypic variability is only partially explained by disease modifiers, such as ApoE4 and environmental factors (35). There is a large kindred of familial AD with a PS1-E280A missense mutation in Antioquia, Colombia, with early onset of disease, language difficulties and in late stages of the disease gait disturbances, seizures and myoclonias (34). Neuropathological studies have shown faster rates of NFT formation, high neuronal loss and increased Aβ_{42} levels with cerebellar pathology (20, 32).

Here we study the neuropathological and biochemical features of PS1-E280A and EOSAD focusing on cerebellar involvement. We show abundant Aβ deposits in the cerebella of PS1-E280A and EOSAD with pTau as a distinctive feature of PS1-E280A.

MATERIALS AND METHODS

Patients and human brain samples

PS1-E280A genealogy was identified 15 years ago and mutation carriers were followed up since then (34). Carriers were identified, and affected patients underwent neurological and neuropsychological characterizations following the consortium to establish a registry for Alzheimer's Disease (CERAD) protocol, National Institute of Neurological and Communicative Disorders and Stroke– Alzheimer's Disease and Related Disorders Association and Diagnostic and Statistical Manual of Mental Disorders, 4th Edition criteria as described (2). Patients were followed up clinically every year upon detection of PS1 mutation, and a detailed clinical database was created from the collected data. Follow-up was carried out until end-stage dementia and death. For neuropathological studies, a rapid autopsy programme was established. We collected postmortem brain tissue of 12 PS1-E280A patients and matched them with 12 EOSAD patients (age of disease onset below the age of 65, average age of disease onset 56.97 years) showing corresponding CERAD and Braak stages (neuropathological analyses were performed by JM, MG and IF) at necropsy according to established guidelines (5, 18) (Table 1). Diagnosis of posterior cortical atrophy was excluded in EOSAD patients following clinical and neuropathological criteria (41). All selected patients had memory complaints as initial symptoms and all of them showed severe neuropathological changes in hippocampus without pronounced pathological involvement of the occipitoparietal region. Procedures were performed following ethical standards of respective institutions. Formalin-fixed samples from frontal cortex and cerebellum were selected for morphological studies. Snap-frozen tissues from identical areas were selected for biochemical analysis.

Genetic analyses

Genomic DNA was extracted from whole blood or brain tissue using standard protocols (19). PS1-E280A and ApoE polymorphism characterization was performed as previously described (35). Briefly, genomic DNA was amplified with the following primers: PS1-S 5′ AACAGCTCAGGAGAGGAATG 3′, PS1-AS 5′ GATGAGACAAGTNCCNTGAA 3′, APOE-S 5′ACAGAAT TCGCCCCGGCCTGGTAcACAC 3′ and APOE-AS 5′TAAGC ITGGCACGGCTGTCCAAGGA 3′. Restriction enzymes BsmI and HhaI were used for characteristic fragments generation for PS1-E280A mutation and ApoE isoforms, respectively. Mutation screening analyses for EOSAD cases were performed by direct sequencing of both strands of polymerase chain reaction-amplified coding exons of PS1 (exons 2–12), PS2 (exons 3–12) and APP (exons 16 and 17), according to published protocols (15). All sporadic cases were confirmed as such after genetic testing.

Neuropathological methods

All morphological analyses were performed on 3-μm-thick deparaffinized sections. For haematoxylin, eosin and Gallyas silver-staining methods, we adhered to published protocols (17). Immunohistochemical staining was performed following pretreatment for antigen retrieval and probed with monoclonal anti-Aβ antibody (6E10, 1:100, Covance, Maidenhead, UK) and anti-pTau antibody (AT8, 1:1500, Thermo Scientific, Rockford, IL, USA). Primary antibodies were visualized using a standard diaminobenzidine streptavidin-biotin horseradish peroxidase method (Sigma Aldrich, Hamburg, Germany). Amyloid plaques were assessed and classified according to standard criteria (13). Cerebral amyloid angiopathy (CAA) was assessed on frontal cortex specimens according to Vonsattel criteria (46). For quantification of the Aβ immunosignal, three representative regions (0.1349 mm^2 each) were analyzed by quantifying the area immunoreactive for Aβ as a percentage of the total area for each image using the AxioVision 4.6 software (Carl Zeiss, Oberkochen, Germany) according to published methods (10). Plaque sizes were determined morphometrically as follows: immunoreactive area for Aβ was divided by the number of identified plaques; values are given in μm^2. For quantification of NFT, AT8 immunoreactive structures resembling tangles (flame-shaped, cone-like or elongated deposits) were quantified as a percentage of total area. Finally, for pTau in the cerebellum, three nonconsecutive sections were cut at a distance of 20 μm and at least three representative regions per section were quantified measuring the area immunoreactive for pTau (in total 0.4047 mm^2).

For double-labelling immunofluorescence and confocal microscopy, sections were stained with a saturated solution of Sudan black B (Merck, Madrid, Spain) for 30 minutes to block autofluorescence, rinsed in 70% ethanol and washed in distilled water. Primary antibodies were: mouse monoclonal AT8, 1:50 (Innogenetics, Gent, Belgium); mouse monoclonal tauSer212, 1:100 (Calbiochem, Barcelona, Spain); mouse monoclonal p38-P, 1:200 (Cell Signaling, Barcelona, Spain); rabbit polyclonal SAPK/JNK-P, 1:100 (Cell Signaling); rabbit polyclonal GSK-3βSer9, 1:100 (Calbiochem); rabbit polyclonal GSK-3β Tyr216, 1:200 (Abcam, Cambridge, UK); rabbit polyclonal anti-Aβ, 1:100 (Dako, Madrid, Spain); and mouse monoclonal anti-Aβ 6F/3D, 1:50 (Dako). Secondary antibodies used for immunofluorescence were Alexa488- and Alexa546-labelled (Molecular Probes, Leiden, the Netherlands) and nuclei were stained with TO-PRO-3-iodide (Molecular Probes). Negative controls

Table 1. Demographic and clinical data. Abbreviations: CERAD = consortium to establish a registry for Alzheimer's Disease; EOSAD = early-onset sporadic Alzheimer's disease; F = female; M = male.

	Age of death	Gender	Disease duration	ApoE genotype	Postmortem Delay	Brain Weight	CERAD	Braak	Memory complaints	Movement disorder	Cerebellar ataxia
1. PS1 E280A											
1	54	F	7	3/3	5.5	1029	C	VI	1	1	1
2	50	F	8	3/3	7.5	987.6	C	VI	1	1	0
3	52	M	8	3/3	4.8	1061.3	C	VI	1	1	1
4	56	M	9	3/3	3.3	941.6	C	VI	1	1	1
5	59	F	20	3/4	3.7	827.2	C	VI	1	1	1
6	67	F	21	3/4	4	581.5	C	VI	1	1	0
7	62	F	13	3/3	4	968.7	C	VI	1	0	0
8	64	F	16	3/3	3	651.7	C	VI	1	1	1
9	48	F	5	3/3	4	886.5	C	VI	1	1	0
10	47	F	10	3/3	2.3	844.9	C	VI	1	1	1
11	55	M	6	4/4	2.8	980.5	C	VI	1	0	0
12	60	F	10	3/3	2.8	768.1	C	VI	1	1	1
2. EOSAD											
13	67	M	12	3/3	5.5	1130	C	VI	1	0	0
14	66	M	9	3/3	9	1050	C	VI	1	0	0
15	72	M	13	3/4	7	980	C	VI	1	0	0
16	66	F	12	3/3	7	1010	C	VI	1	0	0
17	66	F	11	3/3	6.5	810	C	VI	1	0	0
18	68	M	8	3/4	5	1270	C	VI	1	0	0
19	61	M	10	3/3	6.5	1210	C	VI	1	0	0
20	63	F	14	3/3	9	900	C	VI	1	0	0
21	77	F	9	4/4	4.5	1110	C	VI	1	0	0
22	77	F	11	3/4	9.5	1140	C	VI	1	0	0
23	72	F	8	2/4	5	1240	C	VI	1	0	0
24	57	M	12	3/4	4.5	1200	C	VI	1	0	0

Table 2. Variables' comparison between groups. EOSAD = early-onset sporadic Alzheimer's disease; NFT = neurofibrillary tangles; SD = standard deviation.

	Variable	PS1-E280A		EOSAD		Value	*P*
		Mean	SD	Mean	SD		
Demographic	Age of death (years)	56.71	6.38	67.67	6.04	−4.536	0.000*
	Disease duration (years)	11.08	5.32	10.75	1.96	*−0.667*	*0.504*
	Postmortem index (h)	3.98	1.43	6.58	1.79	*−3.27*	*0.001**
	Brain weight (g)	877.38	149.59	1087.5	141.56	−3.534	0.002*
		%		%			
	Male gender	25		50		2.426	0.297
	ApoE4	25		50		7.552	0.109
Frontal cortex	Plaque area (% Total)	36.13	15.84	18.75	8.45	3.335	0.003*
	Plaque size (µm2)	727.89	329.55	463.75	114.01	2.624	0.020*
	Cored plaques	1.69	1.11	1.72	1.24	*−0.262*	*0.794*
	Neuritic plaques	4.69	1.57	4.94	1.99	*−0.348*	*0.728*
	Diffuse plaques	76.94	29.1	49.17	22.87	2.6	0.016*
	$[A\beta 40](ng/\mu g)$	173.12	318.3	27.92	46.23	*−2.829*	*0.005**
	$[A\beta 42](ng/\mu g)$	377.19	155.47	61.71	28.06	6.918	0.000*
	$A\beta 42/ A\beta 40$	10.76	8.47	6.63	4.49	1.489	0.151
	NFT area (% total)	18.32	7.48	31.85	18.27	−2.376	0.027*
	[T181 pTau]	685.24	290.67	300.781	170.74	*−3.175*	*0.001**
Cerebellum	Plaque area (% total)	1.21	0.99	1.72	1.86	−0.841	0.410
	$[A\beta 40](ng/\mu g)$	65.02	87.31	58.91	151.29	*−1.501*	*0.133*
	$[A\beta 42](ng/\mu g)$	103.48	52.45	24.61	32.72	*−3.291*	*0.001**
	$A\beta 42/ A\beta 40$	6.6	6.89	1.41	0.802	*−2.309*	*0.021**
	pTau Area (µm2)	737.46	805.20	0	0	—	—

Italic letters in analysis results represents nonparametric tests, underlined results are χ^2, and statistically significant results are marked with asterisks.

included omission of primary antibodies. Sections were mounted, sealed and examined with a Leica TCS-SL confocal microscope (Wetzlar, Germany).

Ultrastructural analysis

Cerebellar tissues were fixed in glutaraldehyde and chrome-osmium, dehydrated in ethanol and embedded in Epon 812 (Serva Electrophoresis GmbH, Heidelberg, Germany). After polymerization, 1-µm-thick sections were cut, stained with toluidine blue and checked for presence of amyloid plaques. Relevant specimens were further processed for electron microscopy by cutting 60- to 80-nm-thick sections which were contrasted with uranyl acetate and lead solution. Sections were viewed in a LEO EM 912AB electron microscope (Zeiss, Oberkochen, Germany).

Biochemical methods

Sandwich enzyme-linked immunosorbent assay (ELISA) for $A\beta_{40}$, $A\beta_{42}$ and tau pT181 was performed as recommended by the manufacturer (Invitrogen, Carlsbad, CA, USA). Briefly, 100 mg of snap-frozen tissue from frontal cortex and cerebellum were homogenized in 800 µL of 5 M guanidine HCl/50 mM Tris HCl, for Aβ solubilization as reported (25). Homogenate was mixed for 4 h at room temperature, diluted in phosphate-buffered saline/5% bovine serum albumin/0.03% Tween 20 and centrifuged at 16 000 *g* for 20 minutes at 4°C. Supernatant was collected and probed with the ELISA kit for each antigen. Samples were measured at 450 nm in a

Bio-tek µQuant spectrophotometer (Winooski, VT, USA) and expressed as ng/mg of total protein.

Statistical analysis

The data were analyzed using SPSS 17 statistical software (SPSS Inc., Chicago IL, USA). Analyses included Kolmogorov–Smirnov and Shapiro–Wilk tests for normal distribution assessment. For comparison of means, Student's *t*-test (given as t) was applied for two groups if they were normally distributed. For nonparametric comparisons, we applied U-Mann–Whitney (given as Z) for two group comparisons. For association between two variables, Spearman's rho and Pearson's coefficient were applied. Univariate analysis of variance was conducted, testing the following dependent variables: Aβ plaque area, NFT area, Aβ40 concentration, Aβ42 concentration and Aβ42/Aβ40 from frontal cortex and cerebellum. They were tested between groups using disease duration, postmortem delay and ApoE4 status as cofactors. Details on the applied tests for each variable are given in Table 2. Statistical significance of all analyses was determined at $P < 0.05$.

RESULTS

PS1-E280A patients presented with movement disorder and cerebellar symptoms

The demographic data of patients are summarized in Table 1. As expected, PS1-E280A patients had earlier age of onset, died

younger and among demographic data, only brain weights and postmortem delay were significantly lower in PS1-E280A than in EOSAD (Table 2). Even though there were different frequencies in gender and ApoE genotype among groups, these were not statistically significant. Clinical characterization of patients showed that 10 out of 12 PS1-E280A patients presented movement disorders such as parkinsonism or dystonia, and that seven patients showed cerebellar ataxia characterized by ataxic gait or dysdiadochokinesia. Also, 11 out of 12 PS1-E280A patients showed language complaints such as aphasia. There were no movement disorders or cerebellar symptoms diagnosed in the EOSAD group (Table 1).

PS1-E280A shows higher plaque loads and Aβ_{42} concentrations than EOSAD in frontal cortex

We quantified amounts of deposited Aβ and plaque size morphometrically. This analysis showed that PS1-E280A patients had significantly higher plaque loads than EOSAD in frontal cortex (Figure 1A and B). We measured and compared plaque size. PS1-E280A plaques were significantly bigger than those in EOSAD patients (Table 2). When classified as cored, neuritic and diffuse plaques, PS1-E280A diffuse plaques were more numerous, while the number of cored and neuritic plaques was similar in both groups. CAA was assessed in both groups. All PS1-E280A patients were grade 3 in frontal cortex. Only some EOSAD patients showed CAA; three patients were grade 1, two patients were grade 2 and only one patient was classified as grade 3 (data not shown). Biochemical quantification of Aβ_{40} and Aβ_{42} in frontal cortex using ELISA showed significantly more Aβ_{42} in PS1-E280A, when compared with EOSAD (Figure 1C). Concentrations of Aβ_{40} were not as high as Aβ_{42}, yet PS1-E280A patients showed statistically significant higher concentrations than EOSAD. Aβ_{42}/Aβ_{40} ratios showed higher, yet not statistically significant, ratios for PS1-E280A than for EOSAD patients. Disease duration, postmortem delay and ApoE4 status did not influence morphologically or biochemically assessed Aβ pathology.

Higher concentrations of hyperphosphorylated tau in frontal cortex of PS1-E280A patients

Although Braak stages in PS1-E280A and EOSAD patients were identical, PS1-E280A patients showed higher pTau immunosignal in the form of neuropil threads and dystrophic neurites in frontal cortex (Figure 2A) than EOSAD patients who showed higher amounts of classical NFTs (Table 2). PS1-E280A neuropil threads and dystrophic neurites were not necessarily associated to plaques (Figure 3, lines A–C). EOSAD patients presented a pTau pattern characterised predominantly by the presence of neurofibrillary tangles. We used a sandwich ELISA assay for pTau phosphorylated in Threonine 181 to quantify pTau biochemically. PS1-E280A patients showed statistically significant higher T181 pTau concentrations than EOSAD (Figure 2B). pTau concentrations correlated with Aβ_{40} ($r = 0.697$, $P = 0.000$) and Aβ_{42} ($r = 0.677$, $P = 0.000$) concentrations in frontal cortex of both groups. Neither disease duration nor postmortem delay or ApoE4 status influenced morphologically or biochemically assessed pTau pathology.
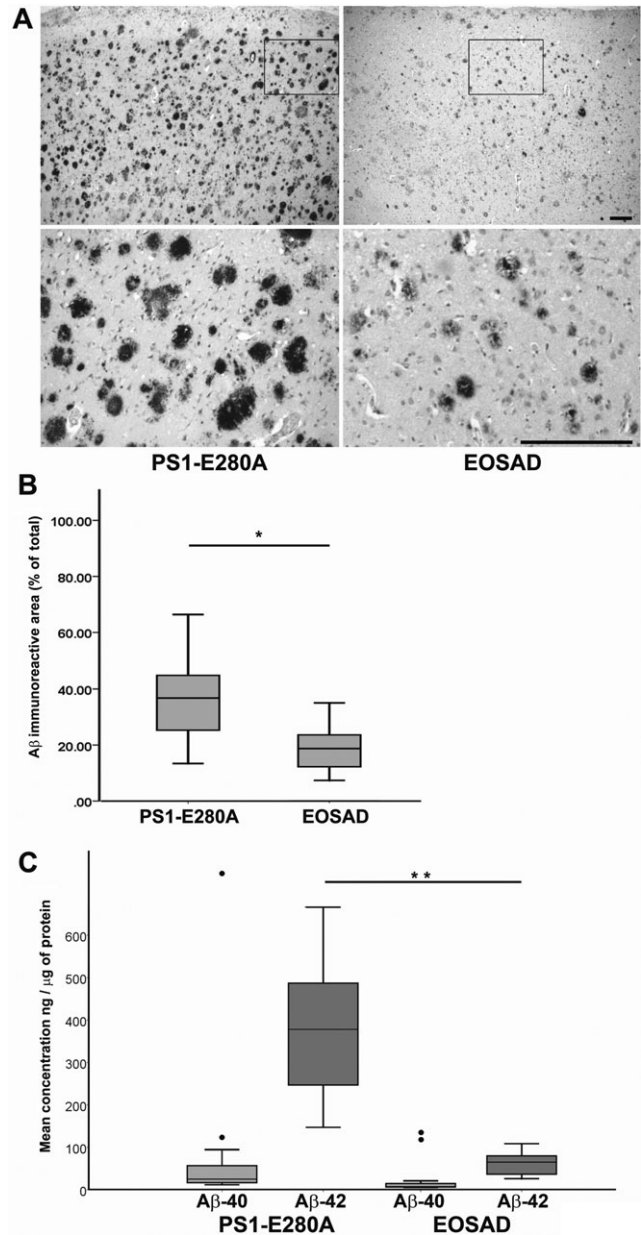
Figure 1. *Abundant deposition of Aβ in frontal cortex of presenilin-1 mutation E280A (PS1-E280A) patients.* **A.** Immunohistochemical staining for Aβ in frontal cortex. PS1-E280A patients showed higher number of diffuse plaques than early-onset sporadic Alzheimer's disease (EOSAD) (scale bar = 100 μm). **B.** Quantification of plaque loads in frontal cortex. PS1-E280A patients showed statistically significant higher loads in PS1-E280A when compared with EOSAD. **C.** Sandwich enzyme-linked immunosorbent assay for Aβ_{40} and Aβ_{42} of frontal cortex. Dots represent outliers. Aβ_{42} levels in PS1-E280A patients were significantly higher than in EOSAD. *$P \leq 0.05$; **$P \leq 0.001$.
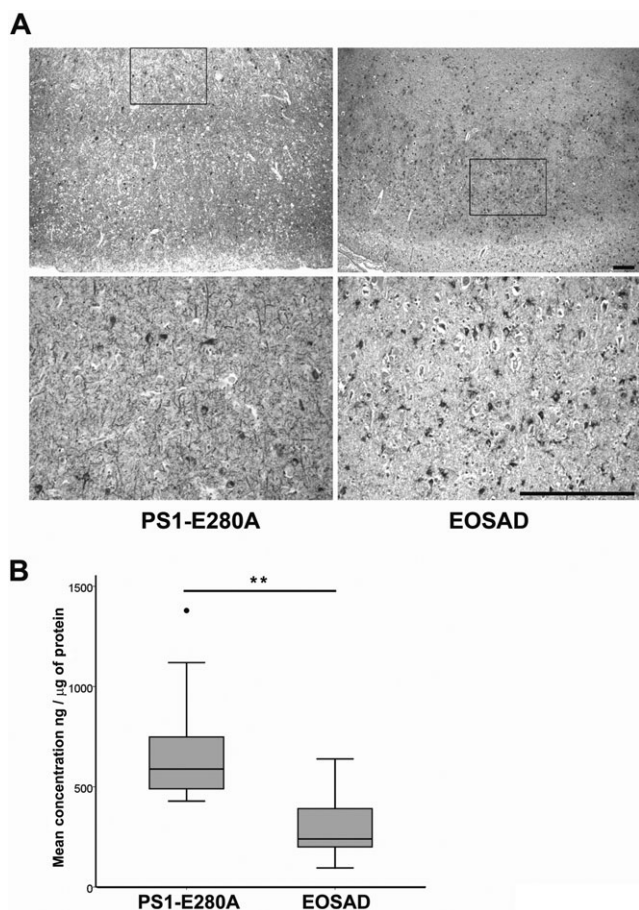
Figure 2. *Increased pTau concentrations in frontal cortex of presenilin-1 mutation E280A (PS1-E280A).* **A.** Immunohistochemical staining for pTau in frontal cortex. Early-onset sporadic Alzheimer's disease (EOSAD) patients showed more typical neurofibrillary tangles and less nonclassical pTau deposits such as dystrophic neurites than PS1-E280A patients (scale bar = 100 μm). **B.** Sandwich enzyme-linked immunosorbent assay for T181 pTau in frontal cortex showing higher concentration of pTau in PS1-E280A patients when compared with EOSAD. A dot represent one outlier; EOSAD patients showed significantly lower levels of pTau. **$P \leq 0.001$.

Cerebellar amyloid pathology in PS1-E280A and EOSAD

The deposition of Aβ in the cerebellum has been reported in familial and severe cases of late-onset AD (28, 42). To further investigate cerebellar Aβ in PS1-E280A, we measured Aβ loads and concentration of $A\beta_{40}$ and $A\beta_{42}$ in cerebella of PS1-E280A and compared these with EOSAD cases. In all PS1-E280A patients, we found abundant deposits of Aβ mostly in the form of diffuse plaques. These were mainly localized in the molecular and Purkinje cell layers. Surprisingly, we found comparable Aβ loads in 11 out of 12 EOSAD patients (Figure 4A and B, Figure S1A). Plaques were also mainly diffuse, but in contrast to PS1-E280A they were found in the Purkinje and granular cell layer. All PS1-E280A patients showed amyloid angiopathy in the cerebellum while only eight

EOSAD patients showed amyloid angiopathy (Figure S1B). Biochemical quantification of $A\beta_{40}$ and $A\beta_{42}$ showed that EOSAD patients with comparable plaque loads in cerebellum have slightly less $A\beta_{40}$ and significantly less $A\beta_{42}$ than PS1-E280A (Figure 4C). There was no correlation between immunohistochemically detected plaque load and biochemically detected $A\beta_{40}$ and $A\beta_{42}$ concentrations (rho = 0.109, $P = 0.566$ and rho = 0.338, $P = 0.068$). The calculated $A\beta_{42}/A\beta_{40}$ ratio was significantly higher in PS1-E280A than in EOSAD patients. Cofactor analysis (disease duration, postmortem delay and ApoE4) showed no influence on Aβ cerebellar pathology.

## Deposition of hyperphosphorylated tau in cerebella of PS1-E280A patients

Because Aβ was detectable in the cerebella of PS1-E280A and EOSAD patients, we evaluated pTau in cerebella morphologically. Unexpectedly, we found deposition of pTau in the molecular layer of cerebella adjacent to Aβ plaques in 11 out of 12 PS1-E280A cases (Figure 5A; Table 2). No pTau was found in the cerebella of EOSAD patients (Figure S2A; Table 2). Ultrastructural analysis of PS1-E280A-affected cerebella showed periaxonal, plaque-associated and isolated NFT in the granular cell layer (Figure 5B). Gallyas staining showed no NFT or pretangle deposits (Figure S2B). EOSAD patients did not show pTau in cerebella.

Differential kinase activation for tau hyperphosphorylation in PS1-E280A cases

Double-labeling immunofluorescence confocal microscopy of frontal cortex and cerebellum showed abundant phospho-tau-immunoreactive neuropil threads but rare dystrophic neurites surrounding amyloid deposits (Figure 3A; data for cerebellum not shown). Because in sporadic AD, tau phosphorylation is achieved by kinases such as GSK-3β, P38-P and SAPK/JNK, we assessed their distribution in frontal cortex and cerebellum. Practically, no association was observed between diffuse plaques and GSK-3βSer9 immunoreactivity (Figure 3B; cerebellum not shown) (14). Immunohistochemistry to GSK-3β in frontal cortex disclosed immunoreactive neurites, some of them in association with core plaques but others not. Interestingly, the anti-GSK-3β antibodies used, including anti-GSK-3β Tyr216 that recognizes the active form and anti-GSK-3β Ser 9 directed against the suspected inactive form of GSK-3β, decorated neurites (Figure S3). P38-P and SAPK/JNK-P immunoreactivity was not observed in association with diffuse plaques in the cerebellum (Figure 6A–F), although these kinases were expressed in cell processes in association with mature amyloid plaques in the frontal cortex (see p38-P in Figure 6G–I) of PS1-E280A cases (Figure 6). GSK-3β, P38-P and SAPK/JNK showed strong immunoreactivity in the frontal cortex of sporadic AD patients (Figure S4).

DISCUSSION

Here we investigated neuropathological features focusing on cerebellar involvement in familial PS1-E280A and EOSAD by correlating genetic, clinical, pathological and biochemical data. PS1-E280A patients showed cerebellar ataxia and movement
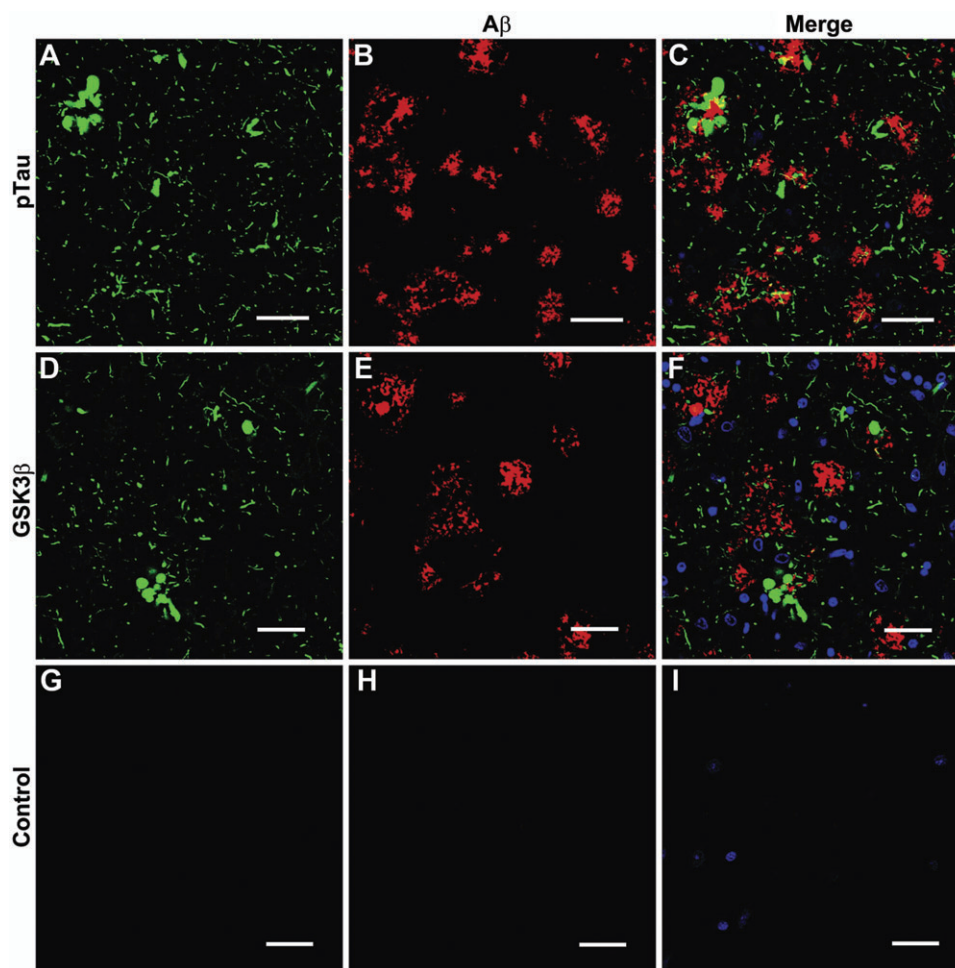
Figure 3. *Rare association of diffuse plaques with pTau and GSK-3β in frontal cortex.* Double-labeling immunofluorescence and confocal microscopy of frontal cortex, for AT8 and Aβ (**A–C**), and GSK-3βSer9 and β-amyloid (**D–F**) in the upper layers of the cerebral cortex. Phospho-tau immunoreactive structures (green in **A** and **C**) were rarely associated with loose Aβ plaques (red in **B** and **C**). GSK-3βSer9 (green in **D** and **F**) was not colocalized with Aβ (red **E** and **F**). **G**, **H** and **I**: sections incubated without the primary antibodies as negative control. **C**, **F** and **I**: merge (scale bar = 50 μm).

disorders; both sets of symptoms were previously described for some PS1 mutations (30). In contrast, EOSAD patients showed no motor symptoms. Regarding neuropathology, we showed that PS1-E280A patients exhibit high plaque load mostly in large diffuse and cotton wool plaques, containing mainly Aβ$_{42}$ in frontal cortex and cerebellum. This is in agreement with previous reports (26, 38, 43). We extended the neuropathological analysis of PS1-E280A patients and described the type and amount of pTau depositions in frontal cortex, which presented differently when compared with similarly affected EOSAD cases. In this study, antibodies used for morphological analyses differ from those used for biochemical analyses, thus measurements are not directly comparable. In PS1-E280A, there were more neuropil threads and dystrophic neurites than NFT when compared with EOSAD. Previously, ELISA pTau quantification of AD brains showed increased amounts when compared with controls (21). Here we showed higher amounts of pTau in the frontal cortex of PS1-E280A patients when compared with EOSAD. A recent study reported no differences between plaque and pTau load in

temporal cortex between EOFAD and late-onset AD with similar Braak stages (48). As PS1-E280A was not included in the study mentioned previously, it is likely that PS1-E280A behaves differently from other PS1 mutations. Differences in amount and pattern of tau phosphorylation can be related with differential kinase involvement. Therefore, we assessed GSK3β and stress kinases in PS1-E280A. There was no involvement of GSK-3β and stress kinases in Tau hyperphosphorylation at the vicinity of diffuse plaques in PS1-E280A cases. Immunoreactive neurites for active GSK-3β were identified but they did not resemble the classical distribution around Aβ plaques for neuritic processes. This is in agreement with recent studies showing decreased PI3K/Akt and GSK3b activation in the presence of mutated PS1 (3). Previously, colocalized activity and expression of kinases GSK3β, SAPK/JNK and p38 with pTau deposits and neurofibrillary tangles in sporadic AD were proposed as supporting arguments for the amyloid cascade hypothesis and subsequent pTau (14). PS1-E280A presents abundant pTau deposits with differential morphology and kinase activity profile compared with EOSAD
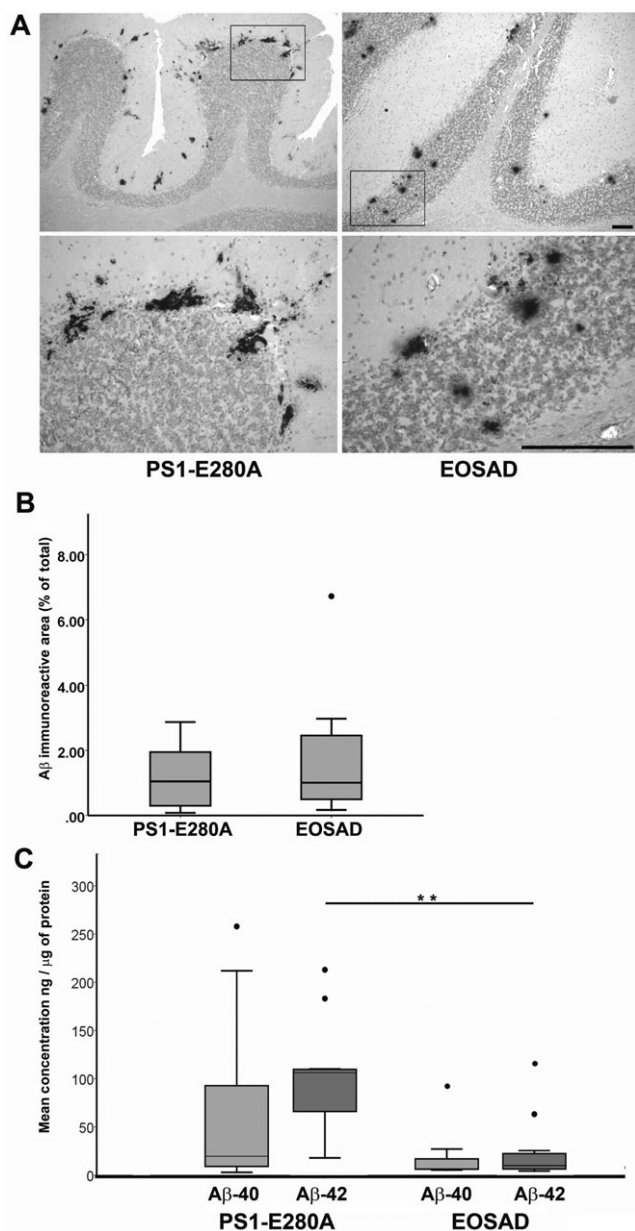
Figure 4. *Deposition of Aβ in cerebella of presenilin-1 mutation E280A (PS1-E280A) and early-onset sporadic Alzheimer's disease (EOSAD).* **A**. Immunohistochemical staining for Aβ of cerebella. All PS1-E280A patients showed amyloid plaques mainly in molecular and Purkinje cell layers. Eleven out of 12 EOSAD patients showed Aβ plaques in Purkinje and granular cell layers (scale bar = 100 μm). **B**. Quantification of plaque loads in cerebellum. PS1-E280A and EOSAD cases showed similar loads. **C**. Sandwich enzyme-linked immunosorbent assay for $Aβ_{40}$ and $Aβ_{42}$ in cerebellum. Dots represent outliers; EOSAD patients showed significantly lower levels of $Aβ_{42}$. *$P \leq 0.05$; **$P \leq 0.001$.

patients; these findings suggest alternative pathways for pTau in this variant of familial AD. However, pTau is also likely to be related here with amyloidogenic pathways because of the observed correlation with $Aβ_{40}$ and $Aβ_{42}$ concentrations.

Some AD patients with PS1 mutations showed diffuse amyloid plaques in the cerebellum (29). We have systematically investigated cerebellar involvement in PS1-E280A and EOSAD. Surprisingly, we detected prominent cerebellar pathology in EOSAD. Thus, it seems that early onset, indicative of an aggressive clinical course, correlated with cerebellar involvement irrespective of familial or sporadic etiology. Therefore, cerebellar pathology might be more common than previously described in sporadic AD. In 2002, Thal *et al* registered 17 AD patients with an age of death above the age of 75 and severe Aβ pathology, and 12 of them presented cerebellar involvement (42). Furthermore, Verdile *et al* compared eight PS1 EOFAD cases carrying six different mutations, with five non-PS1 EOFAD cases and six late onset sporadic AD cases. Cerebellar deposition of Aβ was mainly seen in PS1 EOFAD patients. Moreover, PS1 EOFAD cases showed higher levels of $Aβ_{42}$ in cerebellum when compared with sporadic cases and controls, while non-PS1 EOFAD patients showed similar levels of $Aβ_{40}$ and $Aβ_{42}$ (45). Our study has provided further evidence for cerebellar involvement in AD, arguing against the common practice of employing cerebellum as a negative control in biochemical studies.

We showed a morphological difference in amyloid plaque distribution in the cerebellum of PS1-E280A when compared with the EOSAD. The granular layer was rarely affected in PS1-E280A while molecular and Purkinje cell layers were always affected. In contrast, EOSAD exclusively showed amyloid plaques in the Purkinje and granular cell layers. Our data are in agreement with earlier studies showing Aβ deposition in the molecular layer of patients with PS1 mutations (28). Regarding sporadic AD, our results disagree with a former study indicating deposition of Aβ in molecular layer (42). This difference might be because of the divergence of age of onset between the two studies. The topographical relationship between amyloid plaques and Purkinje cell dendrites in AD has been described (33, 47). It is possible that Purkinje cells play a critical role in Aβ aggregation in cerebellum when APP metabolism is altered because of APP or PS mutations. However, in EOSAD, Aβ aggregation might be influenced by granule cells, Golgi cells or cerebellar afferents. As oligomeric Aβ is associated with excitatory synapses, the distribution Aβ in PS1-E280A and EOSAD is intriguing, as the two main excitatory inputs in the cerebellum are Mossy fiber terminals in the granular layer and climbing fiber synapses of Purkinje cells in the molecular layer (27, 36).

We observed pTau deposits only in the cerebella of PS1-E280A and not in EOSAD. Interestingly, the deposits were not Gallyas-positive, yet could be identified as NFT in ultrastructural analysis. To our knowledge, this is the first demonstration of pTau in the cerebellum of AD patients (28). Only one study in 1989 reported tau deposits in the cerebella of AD patients. Because the employed antibody was non-phosporylation-dependent, it is unclear if the deposits represented pTau (40). Furthermore, we detected extracellular NFTs in the granular layer of PS1-E280A patients, in some cases surrounding amyloid plaques. The association of Aβ plaques and extracellular NFT has been shown before in temporal cortex of AD and Down's syndrome patients (37). On the other hand, extracellular NFT are related with neuronal loss (8) and are increased in the hippocampus of PS1 AD (16). Its presence in the cerebellum of PS1-E280A together with the histological data confirms a distinctive tau-related pathology in these patients.
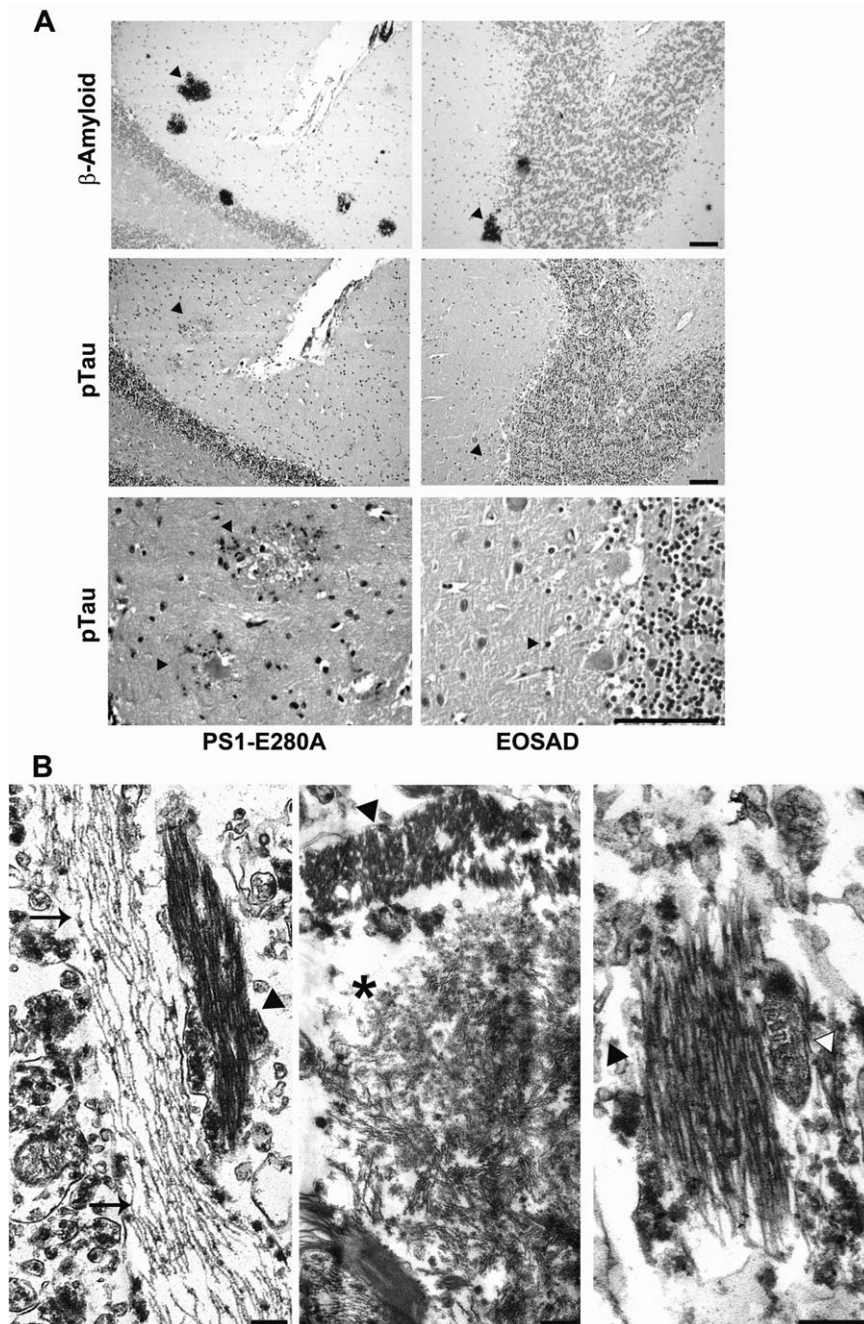
Figure 5. *Cerebellar pTau pathology in presenilin-1 mutation E280A (PS1-E280A).* **A.** Immunohistochemical staining for Aβ and pTau in cerebellum. Arrows indicate plaque and pTau localization in molecular layer of consecutive sections of PS1-E280A (scale bar = 100 μm). **B.** Ultrastructural analysis of cerebellum in PS1-E280A. Longitudinally oriented filamentous structures (neurofibrillary tangles, arrowheads) could be identified alongside axons (arrows), in the direct vicinity of fibrillar compact material (Aβ-plaques, asterisk) and isolated adjacent to dystrophic mitochondria (open triangle) (scale bar = 200 nm). EOSAD = early-onset sporadic Alzheimer's disease.

PS1-E280A carriers suffer from an early and aggressive dementia with wide clinical variability and unpredictable duration of the disease (34), with ApoE and environmental factors as putative disease modifiers (32, 34, 35). Even though both AD groups presented severe Aβ cerebellar pathology, as determined by morphological and biochemical methods, only PS1-E280A patients presented cerebellar symptoms and pTau in the cerebellum. Hence, the presence of high levels of pTau in the cerebella of PS1-E280A patients might represent a disease modifier. Other PS1 mutations, such as P117A (1), M139V, I143T, L166P, Y256S (29) and L288V (11), present with cerebellar ataxia. Further studies are needed to clarify pathophysiological involvement of cerebellar pTau in AD.

ACKNOWLEDGMENTS
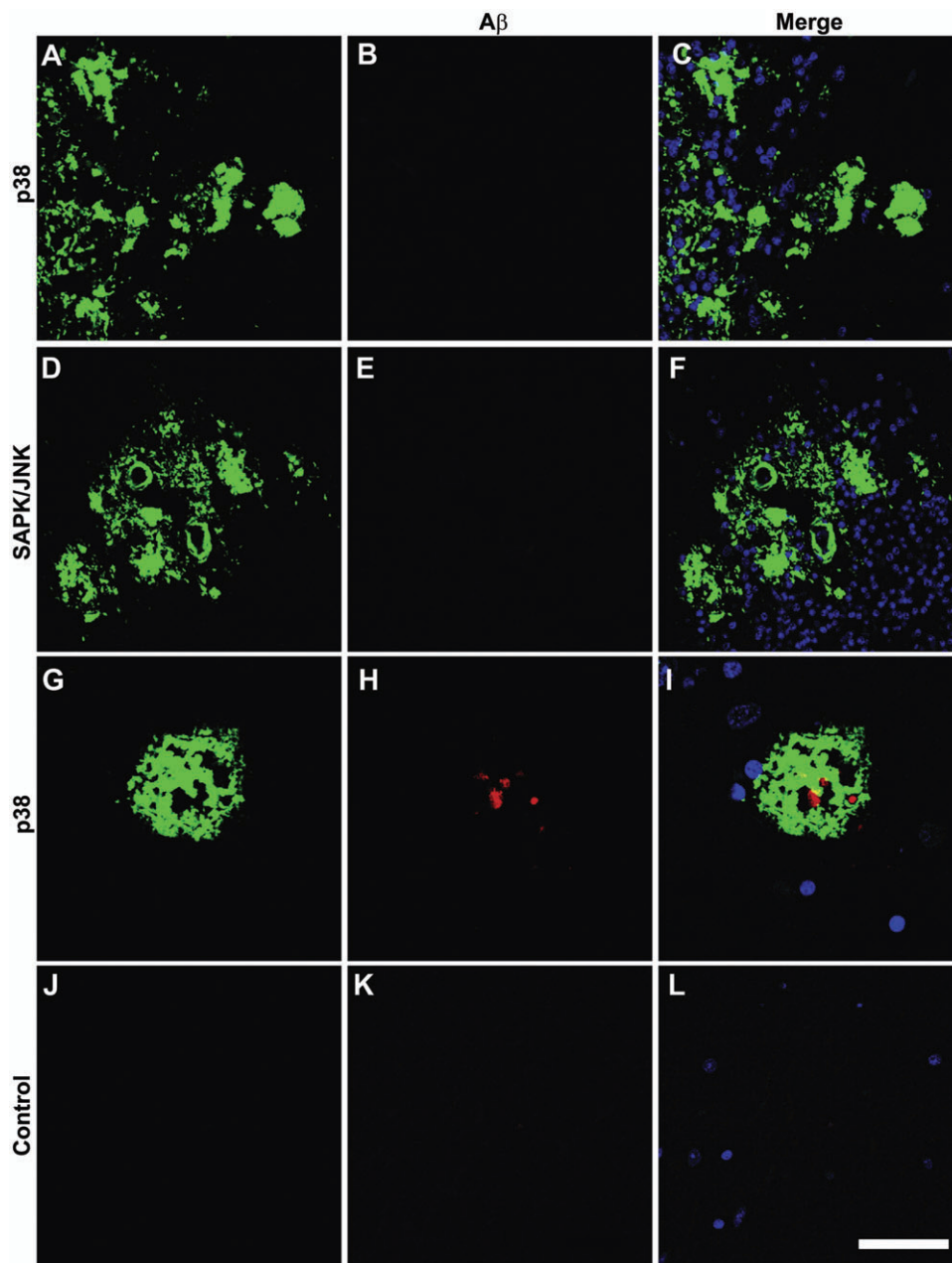
Figure 6. *Lack of stress kinase activity in the cerebellum of presenilin-1 mutation E280A.* Double-labeling immunofluorescence and confocal microscopy to Aβ and p38-P (**A–C**), and Aβ and SAPK/JNK-P (**D–F**) in the cerebellum. No active stress kinase immunostaining was found in the vicinity of amyloid deposits (green in **A**, **C**, **D** and **F**). p38-P expression (**H**, red) is however observed in association with core Aβ plaques (**G**, green) in the frontal cortex. **J–L** incubated without the primary antibodies are used as negative controls. **C**, **F**, **I**, **L**: merge (scale bar = 50 μm).

FUNDING

AUTHOR CONTRIBUTIONS

DSF, JM, CB, CH, IF performed the experiments; MG, DSF, BP, FL, BGM set up the experimental design; DSF, AV, GG, JZ, IF were involved in data and/or patient acquisition; DSF, JM, CB, BP, IF, MG prepared the manuscript.

REFERENCES

1. Anheim M, Hannequin D, Boulay C, Martin C, Campion D, Tranchant C (2007) Ataxic variant of Alzheimer's disease caused by Pro117Ala PSEN1 mutation. *J Neurol Neurosurg Psychiatry* **78**:1414–1415.

2. Ardila A, Lopera F, Rosselli M, Moreno S, Madrigal L, Arango-Lasprilla JC *et al* (2000) Neuropsychological profile of a large kindred with familial Alzheimer's disease caused by the E280A single presenilin-1 mutation. *Arch Clin Neuropsychol* **15**:515–528.

3. Baki L, Neve RL, Shao Z, Shioi J, Georgakopoulos A, Robakis NK (2008) Wild-type but not FAD mutant presenilin-1 prevents neuronal degeneration by promoting phosphatidylinositol 3-kinase neuroprotective signaling. *J Neurosci* **28**:483–490.

4. Bird TD (2008) Genetic aspects of Alzheimer's disease. *Genet Med* **10**:231–239.

5. Braak H, Braak E (1991) Neuropathological staging of Alzheimer's-related changes. *Acta Neuropathol* **82**:239–259.

6. Bu G (2009) Apolipoprotein E and its receptors in Alzheimer's disease: pathways, pathogenesis and therapy. *Nat Rev Neurosci* **10**:333–344.

7. Burns A, Iliffe S (2009) Alzheimer's disease. *BMJ* **338**:b158.

8. Cras P, Smith MA, Richey PL, Siedlak SL, Mulvihill P, Perry G (1995) Extracellular neurofibrillary tangles reflect neuronal loss and provide further evidence of extensive protein cross-linking in Alzheimer's disease. *Acta Neuropathol* **89**:291–295.

9. De Strooper B (2007) Loss-of-function presenilin mutations in Alzheimer's disease. Talking point on the role of presenilin mutations in Alzheimer's disease. *EMBO Rep* **8**:141–146.

10. Debatin L, Streffer J, Geissen M, Matschke J, Aguzzi A, Glatzel M (2008) Association between deposition of beta-amyloid and pathological prion protein in sporadic Creutzfeldt-Jakob disease. *Neurodegener Dis* **5**:347–354.

11. Dermaut B, Kumar-Singh S, De Jonghe C, Cruts M, Lofgren A, Lubke U *et al* (2001) Cerebral amyloid angiopathy is a pathogenic lesion in Alzheimer's disease due to a novel presenilin-1 mutation. *Brain* **124**(Pt 12):2383–2392.

12. Dermaut B, Kumar-Singh S, Engelborghs S, Theuns J, Rademakers R, Saerens J *et al* (2004) A novel presenilin-1 mutation associated with Pick's disease but not beta-amyloid plaques. *Ann Neurol* **55**:617–626.

13. Duyckaerts C, Delatour B, Potier MC (2009) Classification and basic pathology of Alzheimer's disease. *Acta Neuropathol* **118**:5–36.

14. Ferrer I, Gomez-Isla T, Puig B, Freixes M, Ribe E, Dalfo E, Avila J (2005) Current advances on different kinases involved in tau phosphorylation, and implications in Alzheimer's disease and tauopathies. *Curr Alzheimer Res* **2**:3–18.

15. Finckh U, Muller-Thomsen T, Mann U, Eggers C, Marksteiner J, Meins W *et al* (2000) High prevalence of pathogenic mutations in patients with early-onset dementia detected by sequence analyses of four different genes. *Am J Hum Genet* **66**:110–117.

16. Fukutani Y, Sasaki K, Mukai M, Matsubara R, Isaki K, Cairns NJ (1997) Neurons and extracellular neurofibrillary tangles in the hippocampal subdivisions in early-onset familial Alzheimer's disease: a case study. *Psychiatry Clin Neurosci* **51**:227–231.

17. Gallyas F (1971) Silver staining of Alzheimer's neurofibrillary changes by means of physical development. *Acta Morphol Acad Sci Hung* **19**:1–8.

18. Gearing M, Mirra SS, Hedreen JC, Sumi SM, Hansen LA, Heyman A (1995) The Consortium to Establish a Registry for Alzheimer's Disease (CERAD). Part X. Neuropathology confirmation of the clinical diagnosis of Alzheimer's disease. *Neurology* **45**(3 Pt 1): 461–466.

19. Glatzel M, Pekarik V, Luhrs T, Dittami J, Aguzzi A (2002) Analysis of the prion protein in primates reveals a new polymorphism in codon 226 (Y226F). *Biol Chem* **383**:1021–1025.

20. Gomez-Isla T, Growdon WB, McNamara MJ, Nochlin D, Bird TD, Arango JC *et al* (1999) The impact of different presenilin-1 and presenilin-2 mutations on amyloid deposition, neurofibrillary changes and neuronal loss in the familial Alzheimer's disease brain: evidence for other phenotype-modifying factors. *Brain* **122**(Pt 9):1709–1719.

21. Herrmann M, Golombowski S, Krauchi K, Frey P, Mourton-Gilles C, Hulette C *et al* (1999) ELISA quantitation of phosphorylated tau protein in the Alzheimer's disease brain. *Eur Neurol* **42**:205–210.

22. Iqbal K, Grundke-Iqbal I (2008) Alzheimer's neurofibrillary degeneration: significance, etiopathogenesis, therapeutics and prevention. *J Cell Mol Med* **12**:38–55.

23. Jalbert JJ, Daiello LA, Lapane KL (2008) Dementia of the Alzheimer's type. *Epidemiol Rev* **30**:15–34.

24. Jellinger KA, Bancher C (1998) Neuropathology of Alzheimer's disease: a critical update. *J Neural Transm Suppl* **54**:77–95.

25. Johnson-Wood K, Lee M, Motter R, Hu K, Gordon G, Barbour R *et al* (1997) Amyloid precursor protein processing and A beta42 deposition in a transgenic mouse model of Alzheimer's disease. *Proc Natl Acad Sci U S A* **94**:1550–1555.

26. Karlstrom H, Brooks WS, Kwok JB, Broe GA, Kril JJ, McCann H *et al* (2008) Variable phenotype of Alzheimer's disease with spastic paraparesis. *J Neurochem* **104**:573–583.

27. Koffie RM, Meyer-Luehmann M, Hashimoto T, Adams KW, Mielke ML, Garcia-Alloza M *et al* (2009) Oligomeric amyloid beta associates with postsynaptic densities and correlates with excitatory synapse loss near senile plaques. *Proc Natl Acad Sci USA* **106**:4012–4017.

28. Larner AJ (1997) The cerebellum in Alzheimer's disease. *Dement Geriatr Cogn Disord* **8**:203–209.

29. Larner AJ, Doran M (2006) Clinical phenotypic heterogeneity of Alzheimer's disease associated with mutations of the presenilin-1 gene. *J Neurol* **253**:139–158.

30. Larner AJ, Doran M (2009) Genotype-phenotype relationships of presenilin-1 mutations in Alzheimer's disease: an update. *J Alzheimers Dis* **17**:259–265.

31. Larner AJ, Ray PS, Doran M (2007) The R269H mutation in presenilin-1 presenting as late-onset autosomal dominant Alzheimer's disease. *J Neurol Sci* **252**:173–176.

32. Lemere CA, Lopera F, Kosik KS, Lendon CL, Ossa J, Saido TC *et al* (1996) The E280A presenilin-1 Alzheimer's mutation produces increased A beta 42 deposition and severe cerebellar pathology. *Nat Med* **2**:1146–1150.

33. Li YT, Woodruff-Pak DS, Trojanowski JQ (1994) Amyloid plaques in cerebellar cortex and the integrity of Purkinje cell dendrites. *Neurobiol Aging* **15**:1–9.

34. Lopera F, Ardilla A, Martinez A, Madrigal L, Arango-Viana JC, Lemere CA *et al* (1997) Clinical features of early-onset Alzheimer's disease in a large kindred with an E280A presenilin-1 mutation. *JAMA* **277**:793–799.

35. Pastor P, Roe CM, Villegas A, Bedoya G, Chakraverty S, Garcia G *et al* (2003) Apolipoprotein Eepsilon4 modifies Alzheimer's disease onset in an E280A PS1 kindred. *Ann Neurol* **54**:163–169.

36. Rollenhagen A, Lubke JH (2006) The morphology of excitatory central synapses: from structure to function. *Cell Tissue Res* **326**:221–237.

37. Schwab C, Akiyama H, McGeer EG, McGeer PL (1998) Extracellular neurofibrillary tangles are immunopositive for the 40 carboxy-terminal sequence of beta-amyloid protein. *J Neuropathol Exp Neurol* **57**:1131–1137.

38. Shepherd C, McCann H, Halliday GM (2009) Variations in the neuropathology of familial Alzheimer's disease. *Acta Neuropathol* **118**:37–52.

39. Steiner H, Fluhrer R, Haass C (2008) Intramembrane proteolysis by gamma-secretase. *J Biol Chem* **283**:29627–29631.

40. Tabaton M, Cammarata S, Manetto V, Perry G, Mancardi G (1989) Tau-reactive neurofibrillary tangles in cerebellar cortex from patients with Alzheimer's disease. *Neurosci Lett* **103**:259–262.

41. Tang-Wai DF, Graff-Radford NR, Boeve BF, Dickson DW, Parisi JE, Crook R *et al* (2004) Clinical, genetic and neuropathologic characteristics of posterior cortical atrophy. *Neurology* **63**:1168–1174.

42. Thal DR, Rub U, Orantes M, Braak H (2002) Phases of A beta-deposition in the human brain and its relevance for the development of AD. *Neurology* **58**:1791–1800.

43. Van Vickle GD, Esh CL, Kokjohn TA, Patton RL, Kalback WM, Luehrs DC *et al* (2008) Presenilin-1 280Glu - >Ala mutation alters C-terminal APP processing yielding longer abeta peptides: implications for Alzheimer's disease. *Mol Med* **14**:184–194.

44. Verbeek MM, Ruiter DJ, de Waal RM (1997) The role of amyloid in the pathogenesis of Alzheimer's disease. *Biol Chem* **378**:937–950.

45. Verdile G, Gnjec A, Miklossy J, Fonte J, Veurink G, Bates K *et al* (2004) Protein markers for Alzheimer's disease in the frontal cortex and cerebellum. *Neurology* **63**:1385–1392.

46. Vonsattel JP, Myers RH, Hedley-Whyte ET, Ropper AH, Bird ED, Richardson EP Jr (1991) Cerebral amyloid angiopathy without and with cerebral hemorrhages: a comparative histological study. *Ann Neurol* **30**:637–649.

47. Wang HY, D'Andrea MR, Nagele RG (2002) Cerebellar diffuse amyloid plaques are derived from dendritic Abeta42 accumulations in Purkinje cells. *Neurobiol Aging* **23**:213–223.

48. Woodhouse A, Shepherd CE, Sokolova A, Carroll VL, King AE, Halliday GM *et al* (2009) Cytoskeletal alterations differentiate presenilin-1 and sporadic Alzheimer's disease. *Acta Neuropathol* **117**:19–29.

SUPPORTING INFORMATION

Additional Supporting Information may be found in the online version of this article:

Figure S1. Amyloid deposition in cerebellum of PS1-E280A and EOSAD. **A.** Thioflavin S staining in cerebellum of PS1-E280A and EOSAD showed fluorescent plaques in molecular and granular layers respectively. **B.** Immunofluorescence staining against Aβ in the cerebellar cortex showed amyloid angiopathy and diffuse plaques in the molecular layer and between the molecular and granular layers of the cerebellum. There was evidence of amyloid angiopathy in affected vessels.

Figure S2. Dystrophic neurites and pTau in cerebellum of PS1-E280A. **A.** Quantification of pTau immunoreactive area in the cerebellum of PS1-E280A and EOSAD patients. **B.** Immunohistochemistry with AT8 showed dystrophic neurites in the vicinity of an amyloid plaque near Purkinje cells. Gallyas staining of consecutive section showed no related positive structures (scale bar = 50 μm).

Figure S3. Total and active GSK-3β in frontal cortex of PS1-E280A. Shown are immunohistochemical stainings against anti-GSK-3β Ser9 (**A,C**), GSK-3β Tyr216 (**B,D**) of frontal cortex of PS1-E280A (**A,B**) and control (**C,D**). Immunoreactive neurites are marked by arrows. Some of them are related with β-amyloid plaques (asterisks). Staining of the neuropil was negative in control case (scale bar = 40μm).

Figure S4. Kinases immunoreactivity in the frontal cortex of sporadic AD patients. Immunohistochemistry for GSK-3β (**A**), P38-P (**B**) and SAPK/JNK (**C**) in the frontal cortex of sporadic AD patients showing immunoreactive neurites (arrows) (scale bar = 40μm).

Please note: Wiley-Blackwell are not responsible for the content or functionality of any supporting materials supplied by the authors. Any queries (other than missing material) should be directed to the corresponding author for the article.